A Study on the Residual Stress Produced by Metal Cutting

By

Keiji OKUSHIMA* and Yoshiaki KAKINO*

(Received December 28, 1971)

Summary

Residual stresses of machined surface are caused by the mechanical effect and the thermal effect associated with cutting process. Those two effects have been analyzed theoretically using the Finite Element Method and related to X-ray test results of residual stress of carbon steel surface produced by orthogonal cutting.

1. Introduction

Residual stresses in the sub-surface layer of the machined surface are caused by the mechanical effect of the ploughing force which exist at the tool edge, and the thermal effect of the temperature distribution produced in metal cutting. The latter effect is further divided into the thermal stress caused by linear thermal expansion of the work-metal and that caused by volume change due to phase-transformation.

In usual cutting conditions, however, residual stress seldom occurs due to the phase-transformation, because the temperature of the workpiece surface scarecely rises to the temperature of austenic transformation, for example, about 820°C for the 0.45%C plain steel.

For this reason, this paper is concerned with the mechanical effect of the ploughing force which exists at the tool edge and the linear thermal expansion effect due to the temperature distribution produced in metal cutting.

Theoretical analysis is conducted on the residual stress caused by those two effects using the finite element method, and the computed residual stresses are compared to those measured by X-ray diffraction technique.

* Department of Precision Mechanics

2. Theoretical analysis of the residual stress

2-1 Assumptions used in the theoretical analysis

For theoretical analysis of residual stress, a mathematical model is postulated based on several assumptions as follows:

1) The machined surface produced by orthogonal cutting is represented by a semi-infinite flat in which the cutting temperature distribution is applied together with loading of the ploughing force of the tool edge. It is sufficient for the analysis of residual stress to consider only the deformation in the part of the workpiece lower than the finished surface and exclude the deformation in the part removed as the chip.

2) The material retains the plane-strain condition during deformation.

3) The material has a linear work-hardening σ-ϵ relation in the plastic state.

4) The material does not change those properties as modulus of elasticity, work-hardening coefficient, yield stress, Poisson's ratio and linear thermal expansion coefficient when subjected to temperature change.

2.2 The principle of thermal stress and residual stress calculation

Deformations and resulting stresses due to the combination of the mechanical and thermal effects are analyzed by the finite element method. The principle of the analysis is outlined in the following, whereas more details of the finite element method are referred to references 1) and 2).

When the plane-strain condition is retained in the material, the strain $\{\varepsilon_0\}$ of an element produced by thermal expansion is represented by

$$\{\varepsilon_0\} = \begin{Bmatrix} \varepsilon_x \\ \varepsilon_y \\ \gamma_{xy} \end{Bmatrix} = (1+\nu) \begin{Bmatrix} \alpha T \\ \alpha T \\ 0 \end{Bmatrix}$$

where α is the linear thermal expansion coefficient and T is the temperature of the element. The equivalent nodal force $\{f_0\}$ produced by those thermal strains is expressed by the following formula:

$$\{f_0\} = \int_{V_0} [A^{-1}]^t [B]^t [D] \{\varepsilon_0\} \, dV_0$$

In this equation, symbols stand for the followings:

$[A]$ is a 6×6 square matrix, given by

$$[A]=\begin{bmatrix} 1 & x_1 & y_1 & 0 & 0 & 0 \\ 0 & 0 & 0 & 1 & x_1 & y_1 \\ 1 & x_2 & y_2 & 0 & 0 & 0 \\ 0 & 0 & 0 & 1 & x_2 & y_2 \\ 1 & x_3 & y_3 & 0 & 0 & 0 \\ 0 & 0 & 0 & 1 & x_3 & y_3 \end{bmatrix},$$ where (x_i, y_i), $i=1, 2, 3$ represent coordinates of three nodes surrounding the element.

$[B]$ is a 3×6 matrix, given by

$$[B]=\begin{bmatrix} 0 & 1 & 0 & 0 & 0 & 0 \\ 0 & 0 & 0 & 0 & 0 & 1 \\ 0 & 0 & 1 & 0 & 1 & 0 \end{bmatrix}$$

$[D]$ is a 3×3 square matrix, given by

$$[D^e]=\frac{E}{(1+\nu)(1-2\nu)}\begin{bmatrix} 1 & \frac{\nu}{1-\nu} & 0 \\ \frac{\nu}{1-\nu} & 1 & 0 \\ 0 & 0 & \frac{1-2\nu}{2(1-\nu)} \end{bmatrix} \text{ for elastic state}$$

$$[D^p]=2G\begin{bmatrix} \frac{1-\nu}{1-2\nu}-\frac{\sigma_x'^2}{S}, & & \text{Sym} \\ \frac{\nu}{1-2\nu}-\frac{\sigma_x'\sigma_y'}{S}, & \frac{1-\nu}{1-2\nu}-\frac{\sigma_y'^2}{S}, & \\ -\frac{\sigma_x'}{S}\tau_{xy}, & -\frac{\sigma_y'}{S}\tau_{xy}, & \frac{1}{2}-\frac{\tau_{xy}^2}{S} \end{bmatrix} \text{ for elasto-plastic state}$$

where E: modulus of elasticity, G: shearing modulus of elasticity, ν: Poisson's ratio, σ_i': deviatric stress, $S=\frac{2}{3}\bar{\sigma}^2\left(1+\frac{H'}{3G}\right)$, H': work-hardening coefficient, V_0: the volume of the element.

The thermal stresses caused by these nodal forces are calculated in a manner similar to the conventional stress analysis by the finite element method. The present problem, however, should be solved for the situation where some elements are stressed to deform plastically while others are still in elastic conditions. The solution is obtained by a method used by Yamada[2]. By this method, the loads are kept proportional to the distribution pattern of the total loads, and are increased successively by the amount needed to bring only one element in the system to reach plastic state. For every such increment of the external loads, the element found to reach plastic state is regarded as in elasto-plastic stress-strain relation. In this manner, the stresses (σ_{xp}, σ_{yp}, τ_{xyp}) of all elements produced by the total external loads are calculated. When the system is unloaded, the elastic recovering stresses (σ_{xe}, σ_{ye}, τ_{xye}) of all elements are

calculated, assuming a purely elastic recovery. The residual stresses (σ_x'', σ_y'', τ_{xy}'') are given by the differences between the above two sets of stresses, namely:

$$\sigma_x'' = \sigma_{xp} - \sigma_{xe},\ \sigma_y'' = \sigma_{yp} - \sigma_{ye},\ \tau_{xy}'' = \tau_{xyp} - \tau_{xye}.$$

These are the residual stresses developed in the system when the loads are stationary.

In the case of orthogonal cutting, however, the temperature distribution and the mechanical load move along the surface with the advance of the cutting tool. In the finite element simulation, such movement is incorporated by, the use of a successive technique, as follows:

i) The stresses of elements and the deformations of nodal points are calculated for the case in which the load L and the temperature are distributed around the point A as shown in Fig. 1. Then remove the load (also temperature distribution) and find the distribution of the residual stress.

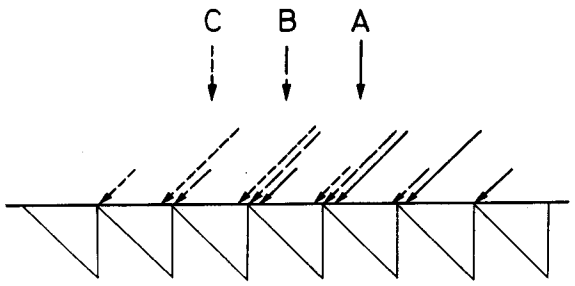

Fig. 1. Illustration on the succesive technique used in computation to incorporate the movement of mechanical load and temperature distribution with the advance of cutting tool.

ii) Assuming that the residual stresses as calculated in the stage i) are the new initial stresses, the stresses and deformations are calculated for the case in which the load L is advanced together with the temperature distribution by one element length from the point A, and is located around the point B.

iii) Step ii) is repeated successively for the cases that the load L and the temperature distribution are distributed around C, D, and so on, until calculated residual stresses converge to constant values.

The outline of computer program used for the calculation of residual stresses is shown in Fig. 2.

2.3 Results of computation and interpretations

The two-dimensional area of 2.4 mm length and 1.2 mm height is assumed in a

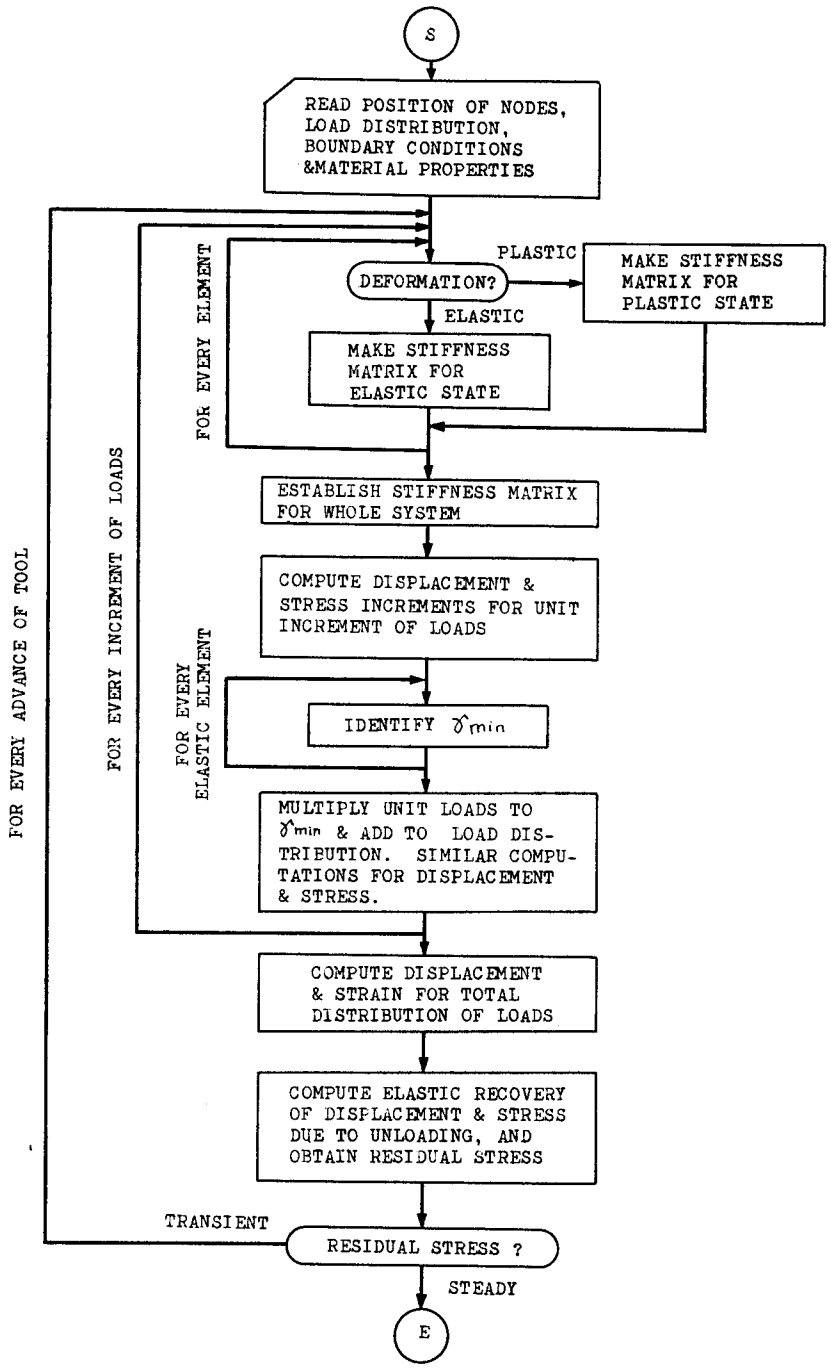

Fig. 2. The outline of computer program used for the calculation of residual stress.

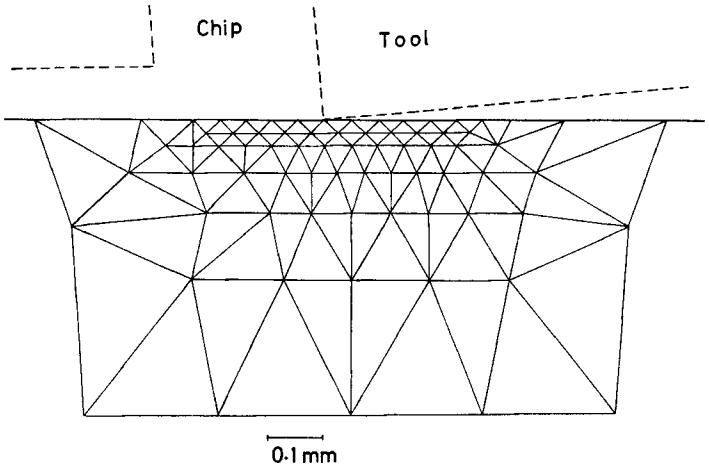

Fig. 3. The divided pattern of two-dimensional area used for the calculation of residual stress.

0.45%C plain steel workpiece, and the area is divided into 160 triangular elements as shown in Fig. 3, the number of nodal points being 105.

The mechanical properties of the steel used in this calculation are as follows:

modulus of elasticity E: 21000 kg/mm^2,
work-hardening coefficient H': 210 kg/mm^2,
yield stress σ_0: 50 kg/mm^2,
Poisson's ratio ν: 0.3,
and linear thermal expansion coefficient α: 0.0000105/°C.

By way of explanation, an example is shown of the residual stress calculated for the orthogonal cutting of the steel at cutting speed 50 m/min, and depth of cut 0.1 mm. Fig. 4(a) shows the distribution of load and temperature at those cutting conditions. This temperature distribution in the workpiece has been calculated with Dutt-Brewer's method[3] using cutting force and other data obtained during the cutting test. As the mechanical load applied to the surface, the ploughing force is assumed exclusively, and the total amount of the ploughing force has been estimated extrapolating the test data of cutting force to zero depth of cut. Then the total amount is assumed to distribute around the cutting edge as shown in Fig. 4(a).

The calculated distributions of residual stress σ_x in cutting direction are shown in Fig. 4(b) along the depth from the surface. In the figure, the residual stress σ_x produced by the combination of the temperature and the mechanical load as Fig. 4(a) is compared to the residual stress by the thermal load alone, and also to that by the mechanical load alone. Distribution of the latter two stresses is found to be tensile

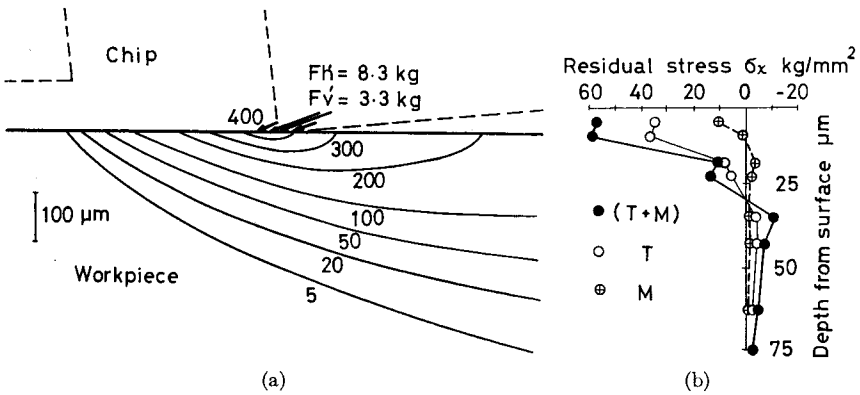

(a) (b)

(a) The distribution of the ploughing force and temperature within the workpiece used for the computation. (Numbers show the temperature in °C)
workpiece: 0.45%C Steel tool: Carbide P10
Cutting speed: 50 m/min depth of cut: 0.1 mm

(b) The computed distributions of the residual stress σ_x in cut diredtion within the machined workpiece.
○ shows the residual stress due to temperature distribution only,
⊕ shows the residual stress due to mechanical force only, and
● shows the residual stress due to combination of the temperature distribution and mechanical force.

Fig. 4. The distribution of loads and the computed residual stress.

in the sub-surface layer. On the contrary, they are slightly compressive in the inner layer which is deeper than 30 μm from the surface. Residaul stress by the combined effects is as high as about 60 kg/mm² tensile in the sub-surface layer, and the value

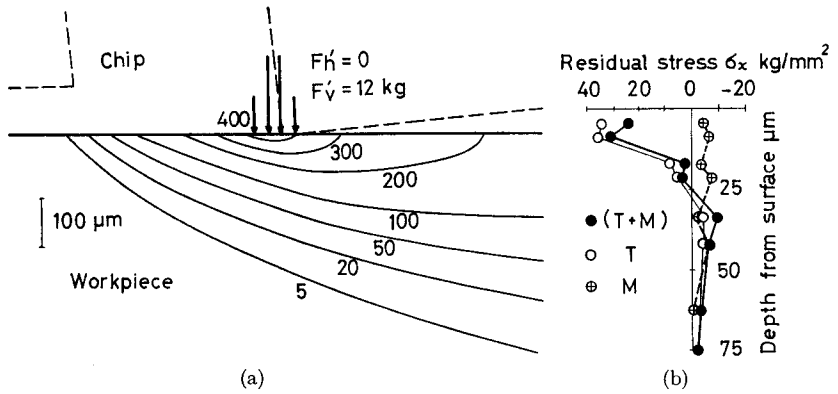

(a) (b)

(a) The distributions of normal loads and temperature
(b) The computed distributions of the residual stress σ_x in cut direction within the machined workpiece.
Symbols are same as Fig. 4 (b).

Fig. 5. Computed example of residual stress for the case ploughing force contains no frictional component but vertical component.

is greater than the simple sum of the two individual cases. It is noted in Fig. 4(a) that the ploughing force loaded in the above case consists of a fairly large frictional force Fh'=8.3 kg, compared to the normal force Fv'=3.3 kg. If the frictional force is omitted, and only normal force Fv'=12 kg is assumed as in Fig. 5(a) together with identical thermal load as before, the tensile residual stress in the sub-surface layer is reduced to that shown in Fig. 5(b). However, as this effect influenced by the increased compressive mechanical load is smaller than the tensile effect by the thermal load, the resultant residual stress is still tensile in Fig. 5(b).

From test data obtained at orthogonal cutting tests performed at various cutting speeds, the temperature distributions inside the work metal have been calculated and the results are shown in Fig. 6. Assuming thermal loads as such, residual stresses due to thermal effect only are calculated and shown in Fig. 7. It is seen from the figure that the sub-surface layer with large tensile residual stress become thinner with

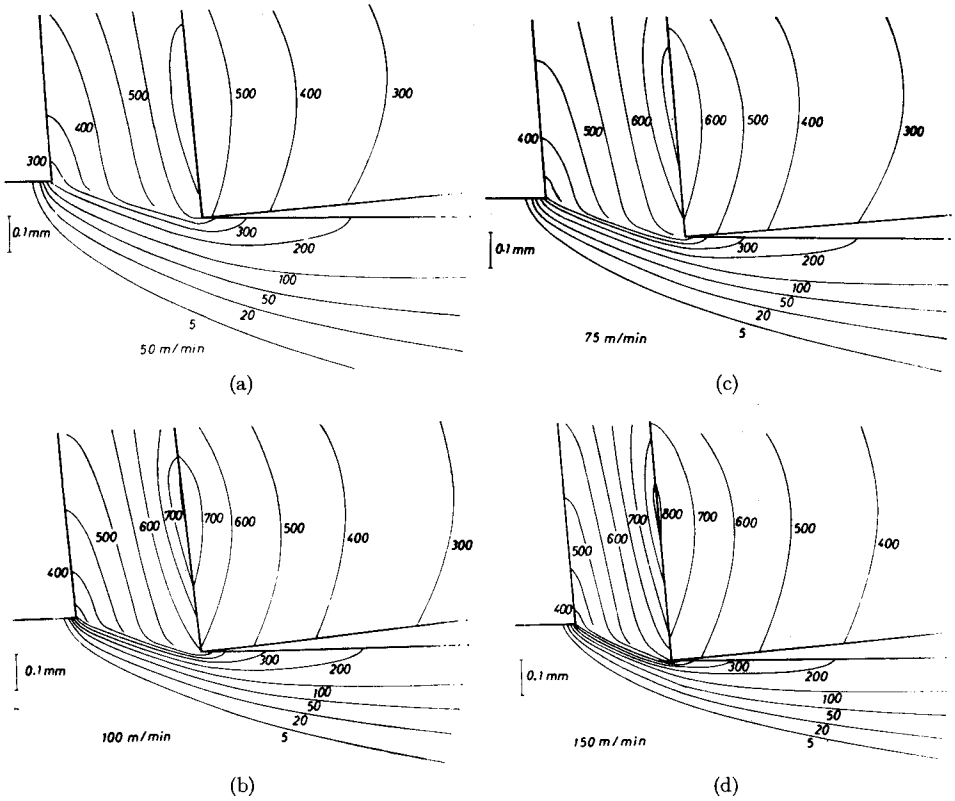

Fig. 6. The computed distributions of temperature within the machined workpiece.
workpiece: 0.45%C steel, tool: carbide P10, rake angle: −5 deg.
relief angle: 5 deg., depth of cut: 0.1 mm, width of cut: 2 mm

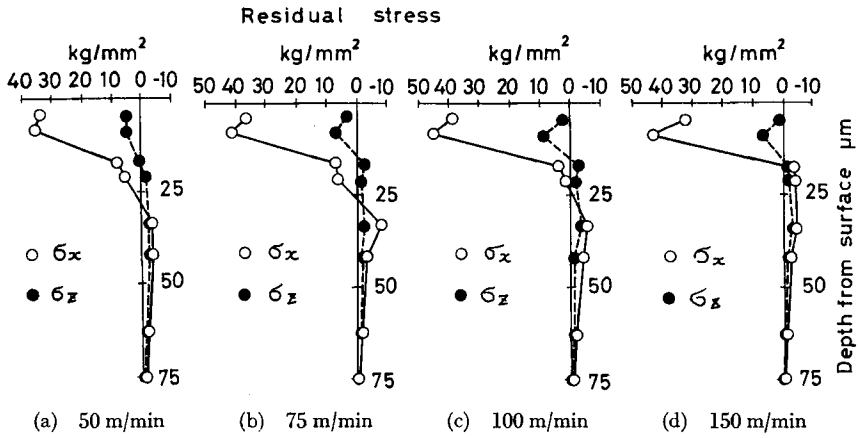

Fig. 7. The computed distributions of the residual stress σ_x in cut direction and σ_z in edge direction within the workpiece due to the temperature as illustrated in Fig. 6.

cutting speed. This phenomena is understood by consulting the change of temperature distribution previously shown in Fig. 6. Namely, the sub-surface layer subjected to high temperature is confined to less depths as cutting speed is raised.

In Fig. 8, effect of the working angle of mechanical load on the residual stresses in the sub-surface layer are shown. In this case, the residual stresses have been calcu-

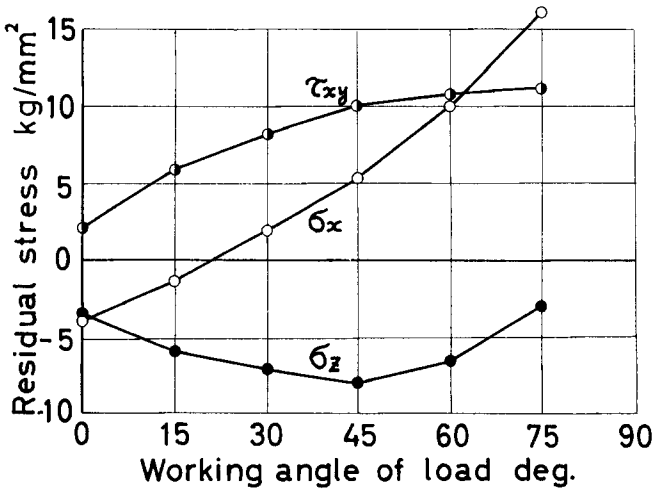

Fig. 8. Effect of the working angle of the ploughing force on the computed residual stresses in the sub-surface layer.

width of cut: 3 mm, total ploughing force: 9 Kg

lated for the mechanical load only. In the figure, a load with greater working angle θ produces greater tensile residual stress σ_x in cut direction. On the contrary, a load with small working angle, for example $\theta=0°$ or 15°, produces compressive residual stress σ_x. The residual stress σ_z in edge direction is always compressive for various working angles. And the shearing residual stress τ holds minimum for $\theta=0°$ and increases with θ.

3. Residual stresses measured by X-ray diffraction technique

3.1 Equipment and procedure for the experiments

The orthogonal cutting tests of 0.45%C plain steel were conducted in order to verify the theoretical analysis developed in the previous section. The conventional cutting tests were also conducted only in order to make comparison with the orthogonal cutting.

For the cutting speeds higher than 50 m/min, tests were conducted using a lathe, and for the cutting speeds lower than 50 m/min, using a shaper. For the study of residual stresses produced by mechanical effect alone, the cutting tests were conducted

Table 1. Chemical compositions, hardness and heat treatments of the work materials tested (0.45%C steel)

Chemical composition (%)								Hardness Vickers	Heat Treatment
C	Si	Mn	S	P	Cu	Ni	Cr		
0.45	0.27	0.68	0.021	0.019	0.09	0.06	0.12	184	860°C, 1 hour annealed

Table 2. Cutting conditions

Workpiece :	0.45%C steel
Tool :	HSS (18-4-1 type) for the shaper test Carbide P10 for the lathe test
Cutting speed :	1.8, 10, 30, 50 m/min for the shaper test, and 75, 100 m/min for the lathe test
Depth of cut :	0.025, 0.05, 0.1, 0.2, 0.3 mm for orthogonal cutting test and 0.125 mm feed for conventional cutting test
Width of cut :	3 mm for orthogonal cutting test, and 2 mm depth of cut for conventional cutting test
rake angle :	25 deg for orthogonal cutting test
relief angle :	5 deg
flank wear width :	0, 0.05, 0.1, 0.2 mm

Table 3. The principal parameters associated with the specific X-ray used.

Test material :	Fe
Lattice constant :	2.8664 Å
Modulus of elasticity :	21000 kg/mm²
Poisson's ratio :	0.3
Specific X-ray	
Anticathode :	Cr
Wave length :	2.28962 Å
Bragg angle of tested material	
(h, k, l) :	(2, 1, 1) 78° 2′ 30″

in the lower cutting speeds to avoid the temperature elevation of the workpiece.

For orthogonal cutting tests, sharp tools of high speed steel finish-ground to 25 deg. rake and 5 deg. relief angles are selected to prevent built-up-edge formation and edge fracture which cause change in effective tool geometries.

Chemical compositions, hardness and heat treatments of the work material are listed in Table 1. The cutting conditions are listed in Table 2.

Residual stress of the finished surface was measured by parallel beam type X-ray diffraction equipment with automatic recording system. The principal parameters associated with the apecific X-ray used are listed in Table 3. X-ray is applied to the finished surface across an area of 2×10 mm², while the specimen is reciprocated across 40 mm length during the meausrement.

3.2 Test results and interpretations

From the X-ray inspection of the surfaces finished by orthogonal cutting at various cutting speeds, it is found that the residual stresses σ_x in cut direction and σ_z in edge direction are both tensile even at the lowest cutting speed of 1.8 m/min, and they increase with the cutting speed, as shown in Fig. 9. Since the temperature elevation of the workpiece is supposedly very small at the 1.8 m/min cutting speed, the tensile residual stress at this cutting speed must have been produced by the mechanical effect. In the orthogonal cutting of the same material, it is found that the working angle θ of the ploughing force from the normal to cut surface direction increases with the cutting speed, and this tendency explains the increase of tensile residual stress with the cutting speed.

In addition to this residual stress by mechanical effect, the tensile stress is produced by thermal load which also increases with the cutting speed.

In the Fig. 9 and the following Fig. 10, the residual stresses σ_z in edge direction,

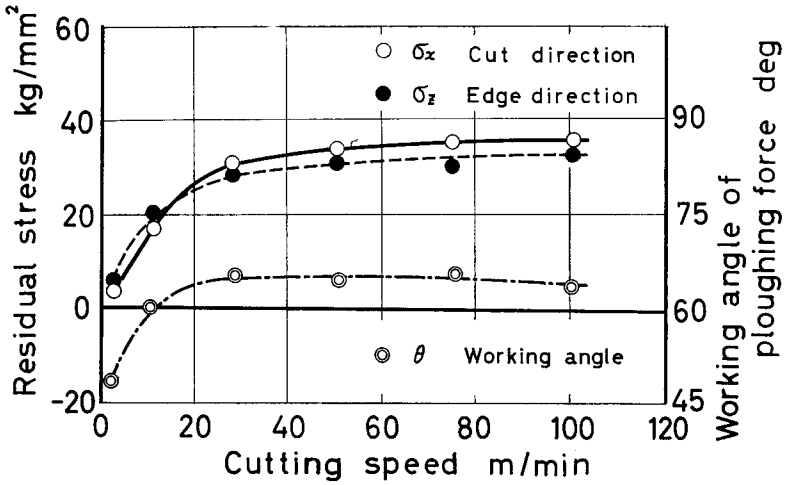

Fig. 9. Effect of cutting speed on the working angle of the ploughing force and the residual stress of the surface machined by orthogonal cutting as measured by X-ray diffraction.

workpiece: 0.45%C steel, tool: carbide P10, rake angle: 25 deg. relief angle: 5 deg., depth of cut: 0.2 mm, width of cut: 3 mm

σ_x in cut direction are both tensile and of similar magnitude. This agrees with experimental results by other authors[4], but contradicts theoretical results previously shown in Fig. 7. The discrepancy is supposedly attributed to the plain strain assumption

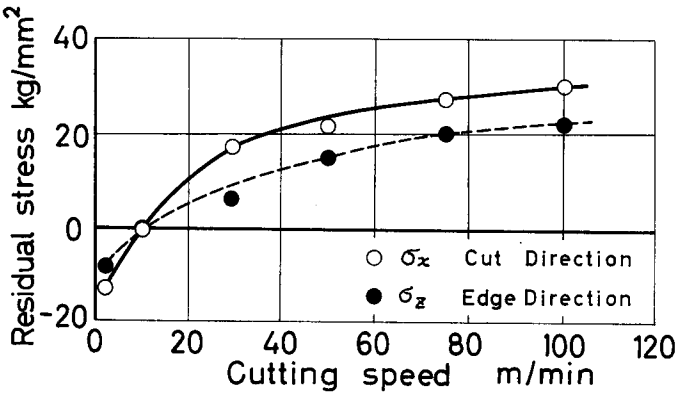

Fig. 10. Relation between the cutting speed and the residual stress of the surface machined by conventional cutting as measured by X-ray diffraction.

workpiece: 0.45%C steel, tool: carbide P10 ε HSS, feed: 0.125 mm/rev
depth of cut: 2 mm, tool geometry: $\gamma=30°$, $\alpha=5°$, $\lambda=-5°$, $\kappa=60°$, $\varepsilon=90°$, $r=0.5$ mm

taken in the theoretical analysis, which is violated in real cutting by occurrence of a flow in the edge direction.

To compare the orthogonal cutting with conventional cutting, the same steel was machined at various cutting speeds, but at 2 mm depth of cut, 0.125 mm/rev feed, and using a 0.5 mm nose radius carbide tool. By the X-ray inspection of the finished surfaces, the residual stresses σ_x and σ_z are both found to be compressive at the lowest cutting speed of 1.8 m/min, and they are almost zero at the cutting speed of 10 m/min. Then they turn tensile at the cutting speeds of 30 m/min and higher, as seen in Fig. 10. The magnitudes of tensile residual stresses σ_x and σ_z are smaller than those in orthogonal cutting by 10 to 20 kg/mm^2. This phenomenon is attributed to the difference in generating process of the machined surface. Namely, in the orthogonal cutting, the machined surface is produced by the major cutting edge, while in conventional cutting it is produced by the minor cutting edge which takes much smaller effective depth of cut at the tool corner. At the last portion of tool-work contact, the surface is only burnished by the tool, and this burnishing effect produces compressive residual stress.

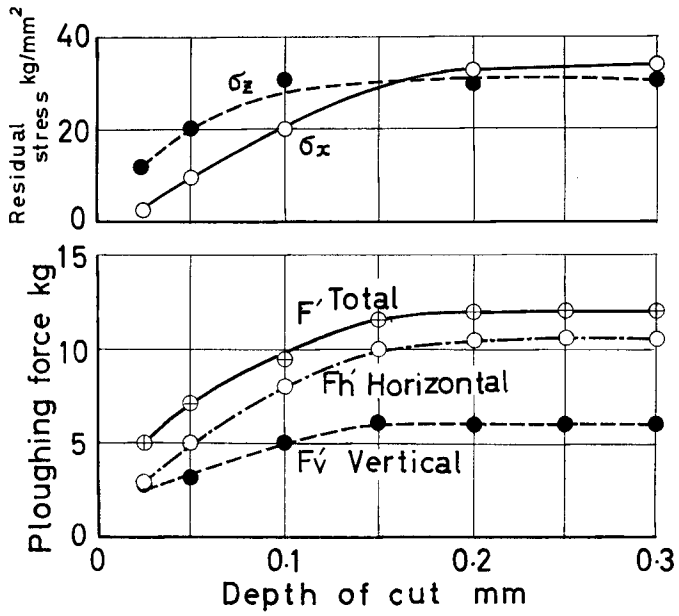

Fig. 11. Relation between the depth of cut and the residual stress of the surface machined by orthogonal cutting as measured by X-ray diffraction (upper), and relation between the depth of cut and the ploughing force (bottom).

workpiece: 0.45%C steel, tool: carbide P10, rake angle: 25 deg. relief angle: 5 deg., cutting speed: 30 m/min, width of cut: 3 mm

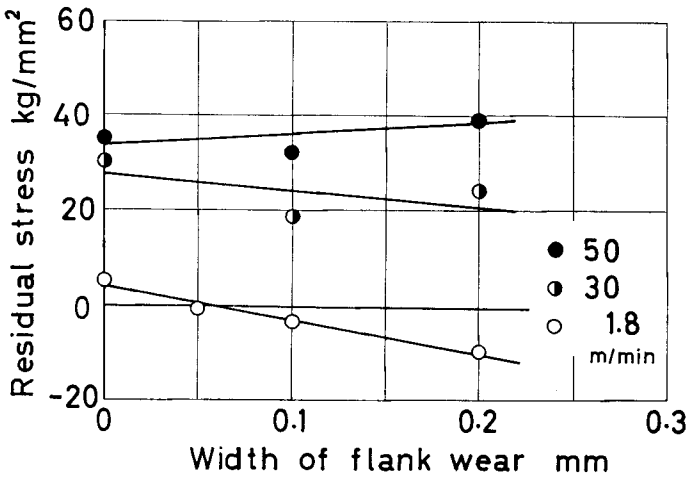

Fig. 12. Effect of flank wear width on the residual stress of the surface machined by orthogonal cutting at various cutting speeds, as measured by X-ray diffraction.

workpiece: 0.45%C steel, tool: carbide P10, rake angle: 25 deg. relief angle: 5 deg., width of cut: 3 mm, depth of cut: 0.2 mm

For various depths of cut in the orthogonal cutting, at 30 m/min cutting speed, the residual stress of the machined surface were obtained as shown in the top graph of Fig. 11. The figure shows that the residual stress σ_x in cut direction is tensile even at 0.025 mm depth of cut, and it increases asymptotically until the depth of cut is increased up to 0.2 mm. This is closely related to the variation of the ploughing force, Fig. 11 bottom. As far as the depth of cut is under 0.2 mm, the deeper depth of cut produces greater ploughing force which converges, however, over 0.2 mm depth of cut.

Orthogonal cutting of the steel was conducted using tools having various flank wear widths at cutting speeds of 1.8, 30, 50 m/min, and the residual stress σ_x was measured. As seen in Fig. 12, the results shows that a tool with wider flank wear produces more compressive residual stress at a low speed cutting due to the burnishing effect, while at a high speed cutting it produces rather tensile residual stress due to the enhanced thermal effect.

4. Conclusions

Residual stresses of the machined surface was investigated from the view point of its generation, and the mechanism was discussed in association with the ploughing force of the tool edge and linear thermal expansion of the work material.

The following conclusions are drawn:

1) Residual stresses in the sub-surface layer of the machined surface are caused by the mechanical effect of the ploughing force which exist at the tool edge and linear thermal expansion effect by the temperature distribution produced in metal cutting. They are not likely to be produced by phase transformation of the material so far as practical metal cutting is concerned.

2) Residual stress caused by mechanical effect, is tensile when working angle θ of mechanical load is large. However it becomes compressive when θ is very small.

3) Residual stress caused by thermal effect is always tensile as far as coolant is not used.

4) In the most cases of practical cutting situations, tensile residual stresses are produced on the machined surface.

Although the effects of residual stress on the functional properties of the machined surface are very complicated, it is at least undesirable to have a large tensile stress in the finished sub-surface layer. This investigation shows that mild cutting conditions, for example, low cutting speed, large vertical ploughing force and small frictional force on the tool relief face, and low temperature elevation are needed to decrease tensile residual stress. This type of situation is utilized in practice in the finish working by a tool having wide front cutting edge at very slow cutting speed, or finish rolling of the surface after machining.

When succeeding finish operation is scheduled after the cutting operation, the magnitude of tensile residual stress is not important, but the depth of sub-surface layer with large tensile residual stress is critical. This can be favorably reduced by a light cutting at a high cutting speed and a small feed rate using tools of high wear-resistance such as TiC cermet tools.

References

1) O. C. Zienkewicz and Y. K. Cheung: The Finite Element Method in Structural and Continuum Mechanics, McGrow Hill (1967).
2) A. Yamada: Stiffness Matrix in Plastic-elastics Problem of Continua, Seisan Kenkyu, Vol. 19, No. 3 (1967), 75 (in Japanese).
3) R. P. Dutt and R. C. Brewer: On the Theoretical Determination of the Temperature Field in Orthogonal Machining, the Intern. J. of Prod. Res., Vol. 4, No. 2 (1965), 91.
4) Y. Ishii: On the Surface Integrity Produced by Cutting, trans. JSME, Vol. 16, No. 53 (1950), 15 (in Japanese).